

Thermal stability up to 800 °C of a Ni–4 wt% Al nanocomposite

L. Zheng · X. Peng · F. Wang

Received: 16 February 2012 / Accepted: 12 April 2012 / Published online: 21 April 2012
© Springer Science+Business Media, LLC 2012

Abstract The thermal stability up to 800 °C of a nanocrystalline (NC) Ni (mean grain size ~ 25 nm) with ~ 4 wt% Al dispersed in the form of ~ 160 -nm-sized particles, which was fabricated by co-electrodeposition from a nickel sulfate bath, has been investigated using differential scanning calorimetry (DSC), transmission electron microscopy (TEM) and X-ray diffraction (XRD). The results showed that microstructural evolution of the composite is temperature dependent, i.e., normal grain growth of the NC Ni, ~ 0.6 wt% Al solution into the Ni matrix and direct reaction between Al and Ni to form Ni₃Al precipitates occurred at ~ 290 , ~ 325 and ~ 575 °C, respectively. The distribution of Al in Ni matrix with temperature is fully discussed.

Introduction

Ni, Ni-based alloy and composite electrodeposits (EDs), normally with ultrafine- or nano-grained structures, are widely used in many established and emerging engineering applications, such as recording heads and soft magnetic disk components, microelectromechanical systems (MEMs) components fabricated by the LIGA process (Lithographic, Galvanoformung, Abformung), parts acquired for repairing nuclear steam generator tubes—ElectrosleeveTM and protective coatings for corrosion, erosion and wear [1–7]. Most of these applications involve high ambient temperature and/or pressure at some stage. For example, the Ni MEM

components, with high-precision micrometer, or smaller, features, are subject to annealing as an essential part of a diffusion-bonding assembly method [2]. The tubes repaired by ElectrosleeveTM are required to operate reliably for long times in high-pressure steam at temperatures up to 650 °C [3, 8]. Also EDs are used to protect substrates against high-temperature corrosion [4–7]. In these circumstances, microstructural changes, such as grain growth, recrystallization, solid solution and reaction, can occur and result in degradation of the associated structure-dependent properties of the EDs. Therefore, in most of these applications, thermal stability is a key concern.

Recently, the thermal stability of pure nanocrystalline (NC) Ni EDs has been extensively investigated, and was reviewed by Hibbard and coworkers in 2002 [9]. The results showed that the abnormal grain growth occurred at a temperature lower than 100 °C, and subsequently rapid normal grain growth occurred at approximately 290 °C [9, 10]. Additions of alloying elements, even in trace amounts, have been shown to significantly improve the thermal stability of Ni matrix EDs [9]. This was suggested to be the result of a solute drag effect. For example, the grain growth temperature was observed to be increased from 260 to 360 °C with the addition of 1.2 wt% P [11]. The effect of alloying with Mn and W was reported to be considerable [12, 13]. Furthermore, if there were some in situ precipitation formed during annealing, the thermal stability of the Ni matrix would be increased because of the Zener drag effect [11–13]. However, there are few publications about the thermal stability of NC Ni matrix composites with an ex situ addition of particles, especially for a Ni matrix plus metal nanoparticles. These may differently behave from in situ precipitates because of some different properties, e.g., the type of particle/matrix interfaces, the particle distribution, concentration and size.

L. Zheng · X. Peng (✉) · F. Wang
State Key Laboratory for Corrosion and Protection,
Institute of Metal Research, Chinese Academy of Sciences,
Shenyang 110016, China
e-mail: xpeng@imr.ac.cn

Recently, Susan and coworkers [14, 15] reported oxidation-resistant alumina-forming Ni–Al composites by co-electrodeposition of Ni matrix and Al microparticles. Using a similar composite electrodeposition technique, we developed a new type of nanocomposites that consisted of an NC Ni matrix and dispersed Al and/or Cr nanoparticles [4–7]. The nanocomposites had enhanced ability to undergo selective oxidation of Cr or Al to form a protective scale of chromia or alumina in a very short initial and transient oxidation stage, compared with materials with the same composition that were either micro-grained alloys or composites having an NC Ni matrix with dispersions of microparticles. Peng [16] attributed the result to two nano-effects of oxidation, i.e., the nanosize effect of particles by which $\text{Al}_2\text{O}_3/\text{Cr}_2\text{O}_3$ nucleated on the ubiquitously distributed particles at/adjacent to the surface of the nanocomposites at the onset of oxidation and a nanosize effect of the Ni-matrix grains by which a rapid linkage of the formed $\text{Al}_2\text{O}_3/\text{Cr}_2\text{O}_3$ nuclei through their lateral growth can be achieved by short-circuit diffusion of Al/Cr atoms through the numerous grain boundaries in the Ni matrix. However, the novel nanocomposites are in a non-equilibrium state and their physical and chemical evolution with temperature and time undoubtedly leads to a variation in their structure and composition, which is expected to in turn to affect the selective oxidation process, particularly the long-term oxidation behavior of the nanocomposites. Accordingly, to study the thermal stability of these nanocomposites, it is essential not only to understand fully the early and stable stage oxidation process but also to tailor new nano- or ultrafine-grained materials with high thermal stability and oxidation resistance in the future. For example, Ni grain growth and Al particle dissolution as well as reaction between Ni and Al are expected to occur for the Ni–Al nanocomposite at high temperatures; however, its structural thermal stability has not been reported. In this work, the thermal stability up to 800 °C of a Ni–Al composite, which was prepared using Al particles in a size close to the nano range, has been investigated.

Experimental

Al particles were added to a sulfate bath containing $150 \text{ g l}^{-1} \text{ NiSO}_4 \cdot 6\text{H}_2\text{O}$, $15 \text{ g l}^{-1} \text{ H}_3\text{BO}_3$, $15 \text{ g l}^{-1} \text{ NH}_4\text{Cl}$, $0.1 \text{ g l}^{-1} \text{ C}_{12}\text{H}_{25}\text{NaSO}_4$ and 1 g l^{-1} saccharin for electrodeposition of the Ni–Al composite using a pulse power. The pulse reversal plating parameters are listed in Table 1. Pure copper (>99.5 %) plate with dimensions $20 \times 20 \times 0.5 \text{ mm}$ and nickel (99.9 %) plate with dimensions $15 \times 10 \times 2 \text{ mm}$ were used as substrates. The Ni–Al composites were $\sim 70\text{-}\mu\text{m}$ thick and contained $\sim 4 \text{ wt}\%$ Al (determined by energy dispersive spectroscopy after

Table 1 Pulse reversal plating parameters

	Cathodic process	Anodic process
Pulse-on-time (ms)	0.1	0.1
Pulse-off-time (ms)	0.4	0.9
Current density (A dm^{-2})	4.7	1.4
Work period (ms)	2	2
Temperature (°C)	30	
Stirring rate (rpm)	170	
pH	5.4	
Plating time (h)	2	

abrading $\sim 5 \mu\text{m}$ from the surface). The material deposited on the copper plate was peeled off for transmission electron microscopy (TEM) and differential scanning calorimetry (DSC) tests, and that on the Ni plate was used for X-ray diffraction (XRD) characterization. The calorimetric investigations were performed in a NETZSCH STA 449C instrument using high-purity argon (99.999 %) as purge gas. The measurements were conducted from room temperature to 800 °C. After cooling to room temperature at a rate of $20 \text{ }^\circ\text{C min}^{-1}$, a second DSC run provided the baseline for data analysis.

Results and discussion

The Al particles used were in the range of 60–400 nm and with a mean size of $\sim 160 \text{ nm}$. The TEM results, given in Fig. 1a, indicated that the particles were dispersed in an NC Ni matrix with a mean grain size of $\sim 25 \text{ nm}$. No microcracks or micropores could be observed in Ni/Al interfaces. The dark-field image presented in Fig. 1b indicates some agglomeration of the finer particles.

Figure 2 shows the DSC curve at a heating rate of $10 \text{ }^\circ\text{C min}^{-1}$. It exhibited two exothermic peaks. A shallow one (P_I) was in the temperature range $254 \sim 339 \text{ }^\circ\text{C}$, with the peak at $290.1 \text{ }^\circ\text{C}$ and heat release of $\sim 8.1 \text{ J g}^{-1}$ (calculated by integrating the peak area). P_I is mainly ascribed to normal grain growth of the NC Ni matrix as extensively reported elsewhere [9, 10, 17]. The peak temperature and amount of heat released are very close to the corresponding values ($\sim 290 \text{ }^\circ\text{C}$ and $\sim 7.1 \text{ J g}^{-1}$) of pure Ni EDs with a similar grain size (20 nm) measured by Wang et al. [17] using DSC at the same heating rate ($10 \text{ }^\circ\text{C min}^{-1}$). Furthermore, according to the Kissinger equation [18]:

$$\ln \frac{B}{T_p^2} = -\frac{E_a}{RT_p} + C, \quad (1)$$

where B , T_p and R are the heating rate, the peak temperature and the gas constant, respectively, the activation energy (E_a) for grain growth can be calculated

Fig. 1 **a** Bright-field image and corresponding electron diffraction pattern of the as-deposited Ni–Al composite and **b** black-field image showing the dispersion of the codeposited Al particles

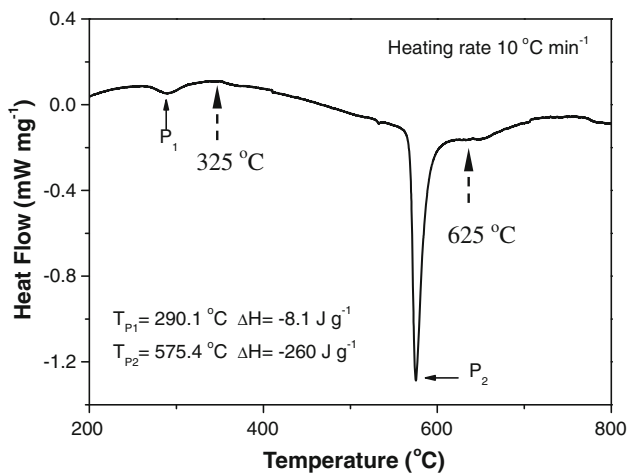
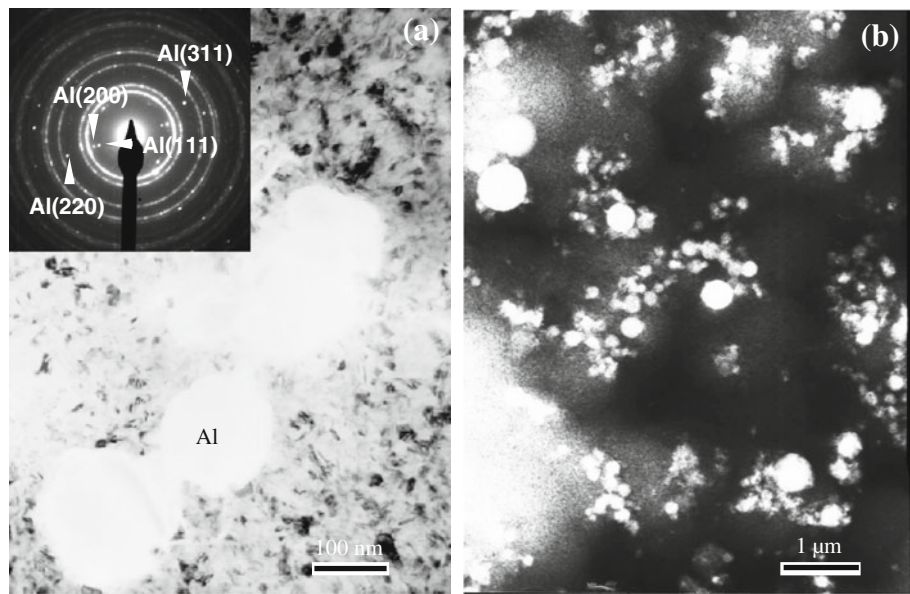


Fig. 2 DSC curve by a heating rate of $10\text{ }^{\circ}\text{C min}^{-1}$ for the as-deposited Ni–4 wt% Al

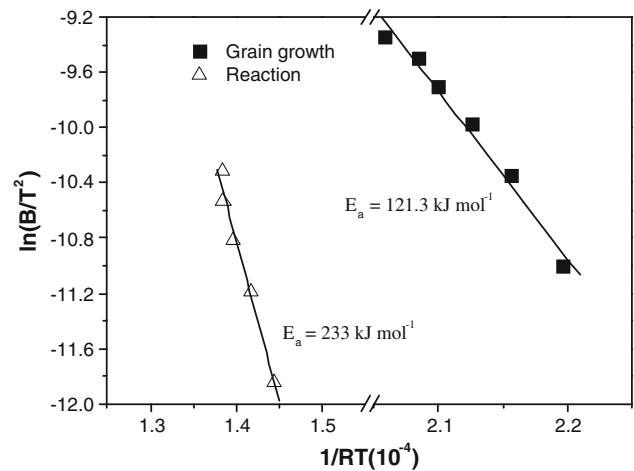


Fig. 3 Kissinger's plot of $\ln(B/T^2)$ versus $1/(RT)$ for grain growth of the nanocrystalline Ni matrix and the reaction between the Al particles and the Ni matrix

to be 121.3 kJ mol^{-1} from the slope of $\ln(B/T^2)$ versus $1/(RT)$ given in Fig. 3. This value is also similar to the E_a (131.5 kJ mol^{-1}) for the pure NC Ni EDs [17]. The results suggest that the presence of the finer 4 wt% Al particles has an insignificant effect on the normal grain growth of NC Ni. The other peak (P_2) was sharp and occurred in the temperature range $394\sim 713\text{ }^{\circ}\text{C}$, with the peak at $575.4\text{ }^{\circ}\text{C}$ and a heat release of $\sim 260\text{ J g}^{-1}$. Such a sharp peak in this temperature range was not found in the non-isothermal DSC scanning of an NC Ni ED [17].

To understand fully the relationships between the exothermic peaks and the microstructural changes, samples were heated in a vacuum system to the temperatures near the end of P_1 ($325\text{ }^{\circ}\text{C}$) and P_2 ($625\text{ }^{\circ}\text{C}$) (as arrowed with the dashed line in Fig. 2) using a similar heating rate to that

of the DSC measurement and then air cooling to room temperature for XRD characterization. Figure 4 shows the XRD patterns of as-deposited and as-annealed samples. In contrast to the as-deposited sample, the width of the Ni peaks decreased after heating to $325\text{ }^{\circ}\text{C}$, which was mainly caused by grain growth of the NC Ni matrix. Additionally, the position of the Ni peaks was shifted toward lower angles (as listed in Table 2). This was because the larger Al atoms (0.143 nm in radius) were incorporated into the Ni lattice (0.124 nm) according to the Bragg equation [19]. Provided that no lattice distortion occurred in the as-deposited state, the lattice constants of Ni and Al were 0.35238 and 0.40494 nm , respectively. The solid solubility of Al (c) was calculated to be $\sim 0.4\text{ wt}\%$ by the Vegard's law (Eq. 2) [20],

$$c = \frac{a - a_1}{a_2 - a_1} \times 100\% \quad (2)$$

where a , a_1 and a_2 are the lattice constants of solid solution, solvent (Ni) and solute (Al), respectively. Intriguingly, the solid solubility of Al in the Ni matrix was much larger than the value, <0.2 wt%, reported by Susan et al. for Ni–7 wt% Al microcomposites composed of a micrometer-sized Ni matrix and Al micro-particles, even though their temperature was 415 °C and their annealing time was much longer [21]. This different particle solubility results from the difference in the size of Ni matrix grains and Al particles. However, we recently found (Zheng et al. unpublished) that although a similar grain growth DSC peak was acquired for an Ni–11.7 wt% Al composite that had a similar Ni matrix nanostructure to that in this study but with dispersions of Al microparticles (mean particle size $\sim 1.4 \mu\text{m}$), no significant XRD line position displacement was seen, even after heating to a much higher temperature of 556 °C. The result demonstrates that the particle size rather than the Ni matrix grain size is the dominant factor for the solution kinetics of Al into the Ni matrix, i.e., finer particles lead to higher solubility. One reason for the result is related to the fact that the thermal stability of the particle decreases with its size, because of an increase of the surface energy. Another reason may be that the Ni matrix in this study during its structural evolution with temperature contained a higher density of defects (such as twins and stacking faults), which increased the solid solubility of Al. Furthermore, the Ni matrix with a more uniform particle dispersion that was achieved by replacing the conventionally used micro-particles with the nearly nano-sized particles [16] had a more homogeneous distribution of Al solid solute atoms. This may be an additional reason for the higher Al solubility.

When the temperature was increased to 625 °C, a significant change in the XRD patterns occurred compared with those at 325 °C (Fig. 4). Ni₃Al peaks emerged, the Al peaks disappeared and the positions of diffraction peaks (200) and (220) of Ni decreased further (see Table 2). This result suggests that the Al solubility was continuously increased from 0.4 to 0.6 wt% and P_2 was mainly caused by solid phase reaction between Al and Ni to form Ni₃Al. Susan et al. [21] found that before the final Ni₃Al phase occurred after heating a Ni–7 wt% Al composites (>1.5- μm -sized particles) to 1,000 °C, an intermediate NiAl phase was formed. The formation of this phase is understandable, because the activation energy of the reaction between Ni and Al to form NiAl is lower than that to form Ni₃Al. The difference in the activation energies is consistent with the fact that the formation temperature of Ni₃Al, 575.4 °C, obtained by DSC in this study is much higher

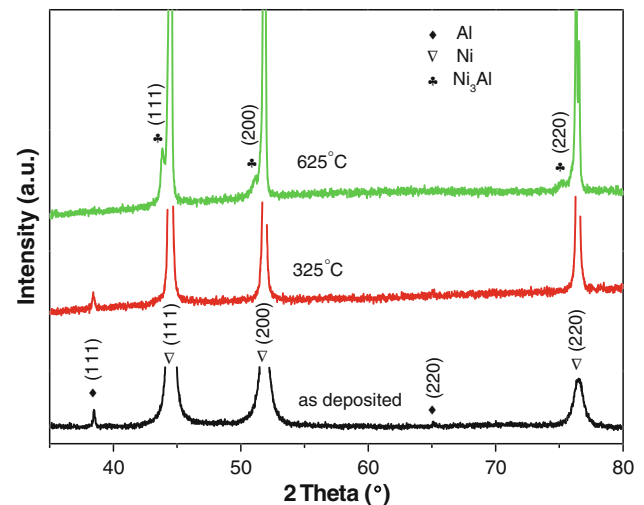


Fig. 4 XRD patterns of the Ni-4 wt% Al composite before and after linearly heated to the desired temperatures with a rate of $10 \text{ }^\circ\text{C min}^{-1}$

than that of NiAl, 532 °C, obtained by DTA by Susan et al. [21]. However, NiAl was not formed in this study, possibly because the rapid dissolution of the finer Al particles into the Ni matrix led to the local amount of Al available for the reaction between Ni and Al to be lower than the critical value for the formation of NiAl but was sufficient for the formation of Ni₃Al. The activation energy for the reaction between Ni and Al to form Ni₃Al was calculated from Eq. 1 to be 233 kJ mol^{-1} . This value is similar to that of 249 kJ mol^{-1} for Ni₃Al phase formation reported by Watanabe et al. [22], but much higher than that for the normal NC Ni grain growth (Fig. 3).

The calculated value of the formation enthalpy of Ni₃Al is $-467.4 \text{ kJ mol}^{-1}$ per mol of Al [23]. The value obtained in this study was $\sim 260 \text{ J g}^{-1}$. From the difference between these two values, the amount of Al consumed by the reaction has been calculated to be $\sim 1.5 \text{ wt\%}$. This value plus the solid solubility ($\sim 0.6 \text{ wt\%}$) of Al in the Ni matrix is $\sim 2.1 \text{ wt\%}$, which is much smaller than the as-codeposited particle content ($\sim 4 \text{ wt\% Al}$). This result suggests that during the DSC scanning, the rest of the Al may segregate to the Ni GBs driven by the lattice misfit strain because of the relatively larger size of the Al atom to Ni. Although significant Ni grain growth occurred during the DSC scanning, the Ni still remained ultrafine-grained

Table 2 2θ of different diffraction peaks of Ni matrix before and after linearly heated to 325 and 625 °C using a rate of $10^\circ\text{C min}^{-1}$

Diffraction peak	(111)	(200)	(220)
As-deposited	44.5201	51.9065	76.5054
After heated to 325 °C	44.4557	51.8143	76.3576
After heated to 625 °C	44.4569	51.7931	76.3253

([6] Zheng et al. unpublished), which makes possible the accommodation of such a large amount of Al at the numerous GBs.

Conclusions

The DSC scanning up to 800 °C of the electrodeposited Ni–4 wt% Al composite shows that the dispersion of the ~160-nm-sized Al particles had no significant effect on the normal grain growth of the ~25-nm-sized Ni (which occurred at 290.1 °C), but changed the composite composition by its reaction with Ni to form Ni₃Al at 575.4 °C. Part of the total as-deposited 4 wt% Al particles formed a ~0.6 wt% solid solution in the Ni and part formed novel Ni₃Al precipitates (~1.5 wt% Al). The rest might exist as segregated atoms at the Ni GBs.

Research highlights

1. Thermal stability of an NC Ni dispersing ultrafine Al particles was investigated.
2. No obvious effect of ~4 wt% Al dispersoids on NC Ni grain growth at 290.1 °C.
3. Reaction of Al particles with Ni to form Ni₃Al at 575.4 °C.
4. Al particles have been converted into solute atoms and Ni₃Al in the DSC scanning.
5. Segregation of part Al at the Ni GB is suggested in the DSC scanning up to 800 °C.

Acknowledgements The work is supported by National Basic Research Program (No. 2010CB934604) of China, Ministry of Science and Technology China.

References

1. Clark D, Wood D, Erb U (1997) *Nanostruct Mater* 9:755
2. Thomas E, David A, Joseph R, Todd R, Steven D (2002) *Metall Mater Trans A* 33:539
3. Palumbo G, Gonzalez F, Brennenstuhl AM, Erb U, Shmayda W, Lichtenberger PC (1997) *Nanostruct Mater* 9:737
4. Zhang Y, Peng X, Wang F (2004) *Mater Lett* 58:1134
5. Zhou Y, Peng X, Wang F (1050) *Scripta Mater* 50(2004):1429
6. Yang X, Peng X, Wang F (2007) *Scripta Mater* 56:891
7. Yang X, Peng X, Wang F (2009) *J Electrochem Soc* 156:C167
8. Viswanathan R, Bakker WJ (2001) *J Mater Eng Perform* 10:81
9. Hibbard G, Erb U, Aust KT, Klement U, Palumbo G (2002) *Mater Sci Forum* 386–388:387
10. Klement U, Erb U, El-Sherik AM, Aust KT (1995) *Mater Sci Eng A* 203:177
11. Mehta SC, Smith DA, Erb U (1995) *Mater Sci Eng A* 204:227
12. Talin AA, Marquis EA, Goods SH, Kelly JJ, Miller MK (2006) *Acta Mater* 54:1935
13. Choi P, Al-Kassab T, Gärtner F, Kreye H, Kirchheim R (2003) *Mater Sci Eng A* 353:74
14. Susan DF, Marder AR (2002) *Oxid Met* 57:131
15. Susan DF, Marder AR (1000) *Oxid Met* 57(2002):159
16. Peng X (2010) *Nanoscale* 2:262
17. Wang N, Wang ZR, Aust KT, Erb U (1997) *Acta Mater* 45:1655
18. Kissinger HE (1957) *Anal Chem* 29:1702
19. Bragg WH (1913) *Nature* 91:477
20. Vegard L (1921) *Z Phys* 5:17
21. Susan DF, Misiolek WZ, Marder AR (2001) *Metall Mater Trans A* 32:379
22. Watanabe M, Horita Z, Sano T, Nemoto M (1994) *Acta Metall Mater* 42:3389
23. Liang YJ, Che YC (1993) *Handbook of inorganic thermodynamic data (in Chinese)*, 1st edn. Northeastern University Press, Shenyang